Since January 2020 Elsevier has created a COVID-19 resource centre with free information in English and Mandarin on the novel coronavirus COVID-19. The COVID-19 resource centre is hosted on Elsevier Connect, the company's public news and information website.

European Journal of Pharmacology 930 (2022) 175169

Contents lists available at ScienceDirect

European Journal of Pharmacology

journal homepage: www.elsevier.com/locate/ejphar

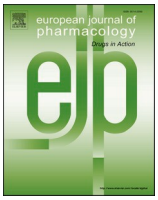

Mast cells promote viral entry of SARS-CoV-2 via formation of chymase/spike protein complex

Shuang Liu [a,*], Yasuyuki Suzuki [a,b,c], Erika Takemasa [a], Ryusuke Watanabe [a], Masaki Mogi [a]

[a] Department of Pharmacology, Ehime University Graduate School of Medicine, 454 Shitsukawa, Toon, Ehime, 791-0295, Japan
[b] Department of Anesthesiology, Saiseikai Matsuyama Hospital, Matsuyama, Japan
[c] Research Division, Saiseikai Research Institute of Health Care and Welfare, Tokyo, Japan

ARTICLE INFO

Keywords:
Mast cell
SARS-CoV-2
Chymase
Spike
Inhibitor

ABSTRACT

The pulmonary pathological findings associated with severe acute respiratory syndrome coronavirus 2 (SARS-CoV-2) result from the release of multiple proinflammatory cytokines, which causes the subsequential damage of the lungs. The current study was undertaken to investigate the responses of mast cells to viral inoculation and their contribution to host defenses from the point of view of viral entry. Pseudovirions, in which the spike glycoprotein of SARS-CoV-2 was incorporated, triggered activation of mast cells, and a mast cell-derived chymase, MCP2, formed a complex with spike protein, which promoted protease-dependent viral entry. According to the quantification results of viral entry, 10 μM quercetin, a mast cell stabilizer, potentially potently inhibited 41.3% of viral entry, while 100 μM chymostatin, which served as a chymase inhibitor, suppressed 52.1% of viral entry, compared to non-treated cells. Study using mast cell-deficient mice showed that the absence of mast cells may influence early viral loading in the upper respiratory tract, which consequently increases the risk of viral invasion into the lower respiratory system. Furthermore, mast cell-deficient mice exhibited ongoing infection in the late phase post-viral inoculation, while clearance of virus-positive cells was observed in wild-type mice. In conclusion, mast cells act as a multifaceted immune modulator that is equipped with both protective effects and pathogenic influences on viral entry of SARS-CoV-2. The utility of mast cell stabilizers and chymase inhibitors in the treatment of SARS-CoV-2-induced acute respiratory syndrome should be optimized regarding the infection stage and the risk of cytokine storm.

1. Introduction

Severe acute respiratory syndrome-related coronavirus 2 (SARS-CoV-2) is a positive-sense, single-stranded RNA-enveloped beta-coronavirus. Gene fragments express structural proteins, which are encoded by the S, E, M and N genes (Chan et al., 2020). A surface glycoprotein, spike, which is encoded by S gene, is an essential component for viral entry of SARS-CoV-2, as well as other beta-coronaviruses (Huang et al., 2020). The spike protein consists of an extracellular N-terminus, a transmembrane domain (TM) anchored in the viral membrane, and a short intracellular-C-terminal segment. The S1 and S2 subunits, which are located on the spike protein following an N-terminus signal peptide, are responsible for receptor binding and membrane fusion, respectively (Xia et al., 2020). In the S1 subunit, a receptor-binding domain (RBD) is capable of folding independently of the rest of the spike protein and contains all structural information for host receptor binding. The S2 subunit consists of a fusion peptide, heptapeptide repeat sequence 1 (HR1), HR2, TM, and cytoplasmic domain. As one of the widely accepted receptor-dependent pathways mediating viral entry, the S protein binds to the target cell via the angiotensin converting enzyme 2 (ACE2) receptor, followed by activation by the host transmembrane protease serine 2 (TMPRSS2) protease and coreceptors, which induce fusion of the virus lipid coat with the cell membrane (Letko et al., 2020).

Mast cells are important sentinel cells in the first line of host defense against viral and bacterial entry. They are strategically placed at sites that interface with the external environment such as skin and mucosal surfaces. SARS-CoV-2 can activate mast cells present in the respiratory tract in the initial stage of the disease (Kempuraj et al., 2020). Mast cell-derived proteases are indicated to be the triggers for the subsequent cytokine storm in the lung, and contribute to pulmonary inflammation and fibrosis (Kritas et al., 2020; Theoharides et al., 2012). Evidence from animal models and non-human primate models also supports that mast

* Corresponding author. Department of Pharmacology, Ehime University Graduate School of Medicine, Shitsukawa, Toon, Ehime, 791-0295, Japan.
E-mail address: liussmzk@m.ehime-u.ac.jp (S. Liu).

https://doi.org/10.1016/j.ejphar.2022.175169
Received 30 March 2022; Received in revised form 6 July 2022; Accepted 21 July 2022
Available online 31 July 2022

cells might be strongly activated during viral invasion, resulting in damage of airway tissue by releasing a series of vasoactive products, including AT II (Morrison et al., 2017). During viral infection, the interactions of mast cells with SARS-CoV-2 are complex and have both detrimental and positive impacts. There is still a massive knowledge gap in this field, as very few works directly focusing on the contribution of mast cells in SARS-CoV-2 infection have been published besides the initial toll-like receptor-dependent activation.

In the present study, we attempted to dissect the mechanisms underlying the interaction of the functions of mast cells, especially focusing on mast cell-derived chymase, with cell entry of SARS-CoV-2. Using a lentiviral pseudotype system in which the spike glycoprotein of SARS-CoV-2 was incorporated into pseudovirions, we were able to study viral entry both *in vitro* and *in vivo* under biosafety level 2 settings (Ou et al., 2020). The interaction between mast cell specific protease and spike protein was observed, and the efficacy of potential inhibitors of viral entry was evaluated.

2. Materials and methods

2.1. Constructs and plasmids

The C9 tagged pcDNA3.1-SARS2-S plasmid encoding SARS-CoV-2 S glycoprotein (NC_045512.2), pLenti6-GFP lentiviral reporter plasmid, VSV-G encoding plasmid, and lentiviral packaging plasmid psPAX2 were obtained from Addgene (Cambridge, MA, USA). A series of truncations was systematically generated. The N-terminal domain of the S1 subunit of the spike protein (pcDNA3.1-SARS2-S1-NTD), RBD region (pcDNA3.1-SARS2-S1-RBD), S1/S2 cleavage region (pcDNA3.1-SARS2-S1-S2), linker region between S1/S2 region and fusion peptide (pcDNA3.1-SARS2-L), and putative fusion peptide region (pcDNA3.1-SARS2-FP) were incrementally removed. The reconstructed plasmids were cleaved by the specific paired restriction enzyme *XbaI/Spe*I at 36 °C for 1 h. The restriction digests of the backbone and insert were separated on a 0.8% agarose gel.

2.2. Production of SARS-CoV-2 S pseudovirions and assessment of viral entry into RBL-2H3 cells

Pseudovirions were produced by co-transfection of HEK-293T cells with psPAX2, pLenti6-GFP, and plasmid - either pcDNA3.1-SARS2-S, pcDNA3.1-SARS2-S1-NTD, pcDNA3.1-SARS2-S1-RBD, pcDNA3.1-SARS2-S1-S2, pcDNA3.1-SARS2-L, pcDNA3.1-SARS2-FP, VSV-G, or empty vector using Lipofectamine® 3000. Titration of pseudovirions in the packaging cell supernatant was monitored using a Lenti-X GoStix Plus cassette (TaKaRa Bio, Tokyo, Japan). After the supernatants were harvested, concentrations of pseudovirus stocks were measured by ultracentrifugation at 130,000×*g* at 4 °C for 2 h. The desired multiplicity of infection (MOI) is 10 for HEK 293T cells and 15 for RBL-2H3 cells.

Rat basophil leukemia (RBL-2H3) cells, a well-established mast cell line, were cultured in Eagle's minimal essential medium (MEM) containing 15% fetal calf serum, 100 units penicillin and 100 μg streptomycin per milliliter at 37 °C in a humidified atmosphere with 5% CO_2. After inoculation of recipient cells with pseudoviruses at 37 °C for 72 h, viral entry was evaluated using a Lenti-X™ provirus quantitation kit (Clontech Laboratories, Mountain View, CA, USA) following the manufacturer's protocol. After virus inoculation, the virus-derived woodchuck hepatitis virus posttranscriptional regulatory element (WPRE), an enhancer contained in retroviral vectors and that is incorporated in the 3′ UTR of nascent transgene transcripts, would integrate into genomic DNA (gDNA) of virus-infected cells. Briefly, genomic DNA was extracted from transduced cells using the provided purification spin columns. Expression of WPRE was quantified by qPCR alongside dilutions of a calibrated provirus control template. After determining the cell number equivalents represented in the gDNA yield using the generic conversion of 6.6 pg gDNA/genome, the integrated copy number in each cell was calculated and the results were expressed as provirus copies/cell.

For immunofluorescence analysis, pseudovirus-inoculated RBL-2H3 cells were fixed at 0 min, 5 min, 30 min, 3 h, 24 h, and 72 h post-pseudovirus inoculation, using 4% paraformaldehyde. After blocking, cells were incubated with a polyclonal rabbit antibody to SARS-CoV-2 spike (Abcam, Tokyo, Japan), and Alex-Fluor 594-conjugated anti-rabbit IgG (Thermofisher, Tokyo, Japan) was used as the secondary antibody. Hoechst 33342 (Dojindo, Kumamoto, Japan) was used for specifically staining the cell nuclei. Images acquired using an all-in-one fluorescence microscope (BZ-X700, Keyence, Tokyo, Japan) at room temperature at 400× magnification were analyzed with ImageJ. The fluorescence intensity of a high-power field was divided by the number of cells to determine the average fluorescence intensity per cell.

As a quick screening index of mast cell activation, β-hexosaminidase release from degranulated mast cells was measured using a previously described method (Liu et al., 2018). After 30 min incubation with thapsigargin (0.5 μM) or pseudovirions, the collected supernatant of RBL-2H3 cells was incubated with 100 μl of 2.5 mM ρ-nitrophenyl-2-deoxy-β-D-glucopyranoside in 50 mM sodium citrated buffer (pH 4.5) at 37 °C for 1 h, and the reaction was stopped by the addition of 20 μl of 2 M potassium hydroxide. Liberated ρ-nitrophenol was measured with a microplate reader at 405 nm.

2.3. Detection of interactions between mast cell-derived proteases and spike protein

RBL-2H3 cells were seeded on a 6-well plate and pseudoviral particles were added to the culture medium. The culture supernatant containing pseudoviral particles and cells was harvested at the indicated time points. PEG-it™ Virus Precipitation Solution (5 ×) (System Biosciences, Palo Alto, CA, USA) was applied to the supernatant to precipitate the suspended viral particles. After centrifugation, the pseudoviral pellets were washed and resuspended using 500 μl RIPA buffer. The infected RBL-2H3 cells were harvested and washed followed by resuspension in 1 ml RIPA buffer.

The protein concentration in the extractions from either culture supernatant or RBL-2H3 cells was determined using the Bio-Rad protein assay. A total of 5 μl of specific antibody to SARS-CoV-2 spike glycoprotein was added to 500 μl protein extract, followed by incubation for 1 h at 4 °C. Then, 30 μl of 1:1 slurry of protein-G Sepharose 4B beads was added to the antibody-extract mixture. After washing, the beads were suspended in 30 μl SDS loading buffer to release the bound proteins. After centrifugation, the supernatants were separated in 12% SDS-PAGE gel and transferred to a polyvinylidene difluoride transfer membrane. After blocking, the blots were incubated with specific antibodies and developed with a chemiluminescent substrate following a standard procedure.

2.4. Investigation of viral entry into HEK-293T cells

To observe the influence of the activation of mast cells on viral entry into HEK-293T cells, the original expansion culture medium of HEK-293T cells, Dulbecco's Modified Eagle medium (DMEM) containing 15% fetal calf serum, 100 units penicillin and 100 μg streptomycin per milliliter, was replaced by the culture supernatants (MEM) of either thapsigargin (TG) (0.5 μM)-treated RBL-2H3 cells or non-treated RBL-2H3 cells before pseudovirus inoculation. Fresh MEM supplemented with 0.5 μM TG was used as a control medium.

In order to investigate the inhibitory efficacy of potential mast cell stabilizers and chymase inhibitors on viral entry, HEK-293T cells were co-cultured with RBL-2H3 cells. HEK-293T cells were seeded directly onto the plastic surfaces of a 24-well plate and cultured in Dulbecco's Modified Eagle medium containing 15% fetal calf serum, 100 units penicillin, and 100 μg streptomycin per milliliter. RBL-2H3 cells were replated at 5 × $10^5/cm^2$ on top of a floating atelocollagen membrane insert (Koken Co., Tokyo, Japan). After incubation at 37 °C with 5% CO_2

for 24 h, the insert was plated upside down on the culture plate.

RBL-2H3 cell-cocultured HEK-293T cells were pretreated with either a mast cell degranulation suppressor (quercetin) or potential chymase inhibitors (chymostatin and Bowman-Birk protease inhibitor (BBI)). The effects of the inhibitors on the viability of both HEK-293T cells and RBL-2H3 cells was analyzed using a Cell Counting Kit-8 (Dojindo, Tokyo, Japan) according to the manufacturer's instruction. The concentrations at which the inhibitors were used in *in vitro* viral entry studies with a

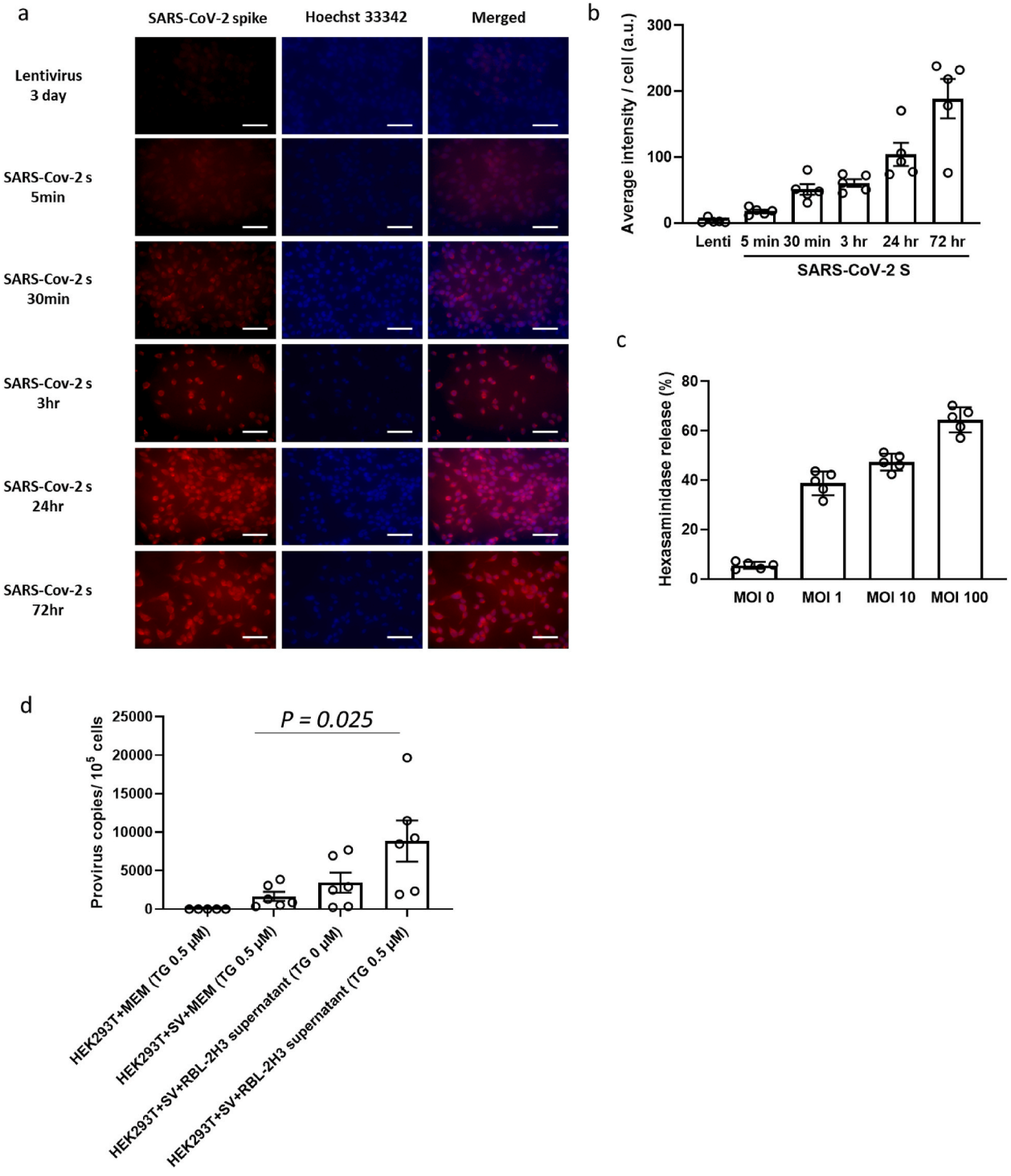

Fig. 1. Pseudovirion inoculation triggers mast cell activation and promotes viral entry. (a) Expression of SARS-CoV-2 spike glycoprotein in pseudovirus-inoculated RBL-2H3 cells at 0 min, 5 min, 30 min, 3 h, 24 h, and 72 h post viral inoculation. Lentivirus-infected cells were used as control at 72 h post-inoculation. (b) Normalized fluorescence signal of SARS-CoV-2 spike using Hoechst 33342. Cells were examined by fluorescence microscopy, and fluorescence intensity of a high-power field was divided by the number of cells to determine the fluorescence intensity per cell (n = 5). (c) Dose-response of hexosaminidase net release trigged by SARS-CoV-2 S inoculation at indicated MOI (n = 5). (d) Viral entry of SARS-CoV-2 S into HEK293 T cells cocultured in 0.5 μM thapsigargin (TG)-supplemented MEM, SARS-CoV-2 S pseudovirion-containing TG (0.5 μM)- supplemented MEM, SARS-CoV-2 S pseudovirion-containing non-treated RBL-2H3 cell culture supernatant, or SARS-CoV-2 S pseudovirion-containing TG (0.5 μM)-treated RBL-2H3 cell culture supernatant. The number of integrated provirus copies in cells was determined 72 h post-inoculation (n = 6). Values are presented as the scatter plot of individual values with mean ± SD.

coculture system were determined on the basis of solubility, cell viability, and inhibition constant (He et al., 1999).

The cells were pre-treated with the inhibitor for 1 h at 37 °C, then spin-inoculated with pseudovirions in the presence of inhibitor at 1200×*g* for 30 min. After 6 h incubation in the presence of inhibitors, the cells were fed fresh medium without inhibitor. After incubation of pseudoviruses with recipient cells at 37 °C for 72 h, the membrane inserts were removed, and viral entry was evaluated using a Lenti-X™ provirus quantitation kit as described above.

2.5. Observation of viral entry into murine respiratory tract in vivo

Male mast cell-deficient WBB6F1/Kit-*Kit^{W}/Kit$^{W\text{-}v}$* mice and C57BL/6JJms mice were used (8 weeks old, S.L.C. Japan, Shizuoka, Japan). All animals were housed at a constant temperature of 22 ± 2 °C with humidity of 55 ± 10% with an automatically controlled 12:12 h light-dark cycle. Animal care and research protocols were in accordance with the principles and guidelines of the Animal Care Committee of Ehime University and were approved by the Ehime University Committee for Animal Research (approval No. 05KI43–1.16).

Mouse infection studies were performed in an animal biosafety level 2 facility. Mice were lightly sedated with isoflurane and inoculated intranasally with 20 μL SARS-CoV-2 pseudovirions (5×10^6 TCID50) or chymase-pretreated SARS-CoV-2 pseudovirions. For MCP2 pretreatment, SARS-CoV-2 S pseudovirions were preincubated with recombinant rat MCP2 (Cusabio, Houston, TX, USA), which was activated by 10 μg/ml activated rat cathepsin C/DPPI (Bio-techne Japan, Tokyo, Japan) according to manufacturer's instructions, for 1 h at 37 °C before inoculation. On day 3 and day 7 after viral inoculation, the number of integrated provirus copies in the upper and lower respiratory tract was determined using a Lenti-X Provirus Quantitation Kit as described above in the *in vitro* viral entry experiments. The final results are expressed as provirus copies/cell.

2.6. Statistical analysis

The sample distributions were analyzed using the Kolmogorov-Smirnov test. Pair-wise comparisons were performed using two-tailed Student's t-test to evaluate the statistical significance of differences in viral entry into HEK-293T cells or RBL-2H3 cells *in vitro* and *in vivo*. The criterion for statistical significance was $P < 0.05$. Data were analyzed using GraphPad Prism 9 (GraphPad Software, La Jolla, CA).

3. Results

3.1. SARS-CoV-2 S pseudovirions enter and activate RBL-2H3 cells

SARS-CoV-2 S pseudovirions readily infected RBL-2H3 cells. An increase in colocalization of SARS-CoV-2 S and RBL-2H3 cells was demonstrated in a time-dependent manner (Fig. 1a and b). We then examined the effect of SARS-CoV-2 S pseudovirion infection on mast cell degranulation. According to the results of measurement of released β-hexosaminidase, which is a prototype lysosomal hydrolase known to be stored in the vesicles and has been used as a hallmark of mast cell degranulation, the infection of SARS-CoV-2 S pseudovirions alone can induce the activation and degranulation of mast cells. At 30 min after viral inoculation, the release of β-hexosaminidase from activated RBL-2H3 cells was observed in a dose-dependent manner (Fig. 1c).

How do the released pre-stored intracellular mediators influence SARS-CoV-2 entry into cells? To pursue the possible impact of soluble mediators released from virus-activated mast cells, degranulation of RBL-2H3 cells was triggered by application of TG, which is a sarcoplasmic/endoplasmic reticulum Ca^{2+}-ATPase pump inhibitor which activates RBL-2H3 cells to a level comparable to that induced by SARS-CoV-2 S pseudovirions (Liu et al., 2016). The supernatant containing the released mediators from RBL-2H3 cells was collected and subsequently used for HEK-293 T cell culture. As shown in Fig. 1d, compared to cells cultured in TG-containing MEM, viral entry was 5.33-fold higher ($P = 0.025$) in HEK-293 T cells cultured in RBL-2H3 cell-derived mediator-containing MEM. Taken together, these results demonstrated that viral entry of SARS-CoV-2 S pseudovirions can directly activate mast cells. Moreover, mast cell-derived soluble factors may contribute to viral entry into other cells.

3.2. Mast cell-derived chymase interacts with SARS-CoV-2 S

The contribution of mast cells to viral entry allows us to tackle the question of which mast cell-derived soluble mediator could act as a potential effector of SARS-CoV-2 S pseudovirions. Given the current acknowledgment of essential processes in SARS-CoV-2 entry, including binding to ACEs and priming by TMPRSS2, proteases released from mast cells could be candidates that potentially enhance viral entry. The interactions between spike protein and mast cell protease 2 (MCP2) or tryptase were investigated. We noticed that the MCP2 signal, but not the tryptase signal, appeared to be enriched in spike-immunoprecipitated blots (Fig. 2a). The spike/MCP2 complex was rapidly formed after viral inoculation and gradually decreased in a time-dependent manner (Fig. 2b).

To elucidate the possible binding/interaction sites on spike and MCP2, a series of spike truncations was generated. The N-terminal domain, RBD region, S1/S2 cleavage region, linker region between S1/S2 region and fusion peptide, and a putative fusion peptide region were incrementally removed up to the predicted HR and transmembrane region (Fig. 2c and d). After viral inoculation, MCP2 was co-immunoprecipitated with wild-type C9-tagged spike, as well as with a spike truncation that included the N-terminal domain and RBD region, but not with the S1/S cleavage region, the linker region between S1/S2 region and fusion peptide truncation, and the fusion peptide truncation. These results indicated that the S1/S2 cleavage region is necessary for MCP2 to bind spike.

The truncated spike-encoding plasmid was then used for the production of pseudovirions, and their infective ability in RBL-2H3 cells was evaluated. Pseudovirions with wild-type spike readily infected the cells, and the entry ability remained in pseudovirions with a spike truncation of the N-terminal domain and RBD region, but not with other truncated spikes. Interestingly, a significant decrease in cell entry ability of pseudovirions with S1/S2-truncated spike, in which hydrophobic fusion peptide is completely exposed, was also observed. These results indicate that the S1/S2 cleavage site, which has potential binding ability to MCP2, could be essential for viral entry.

3.3. Efficacy of mast cell inhibitors against viral entry of SARS-CoV-2 S pseudovirions

We then investigated potential inhibitors of mast cell activation and the action of MCP2 on viral entry of SARS-CoV-2 pseudovirions (Fig. 3). Quercetin, which is normally regarded as an anti-inflammatory agent that reversibly inhibits stimulatory signals and exocytosis in RBL-2H3 cells, was applied to a RBL-2H3 cell-HEK293 T cell coculture system (Senyshyn et al., 1998). According to the quantification results of viral entry, 1-h preincubation with 10 μM quercetin inhibited 41.3% of viral entry into HEK 293 T cells ($P = 0.045$) without influencing cell viability, compared to non-treated cells. Similar blocking effects on viral entry were also observed in chymostatin-administered cells. Compared to non-treated cells, the suppression of 52.1% on viral entry was detected in 100 μM chymostain-treated cells ($P = 0.035$). Conversely, BBI, which is reported to be a highly effective inhibitor of human mast cell chymase (Ware et al., 1997), did not influence viral entry into HEK 293 T cells.

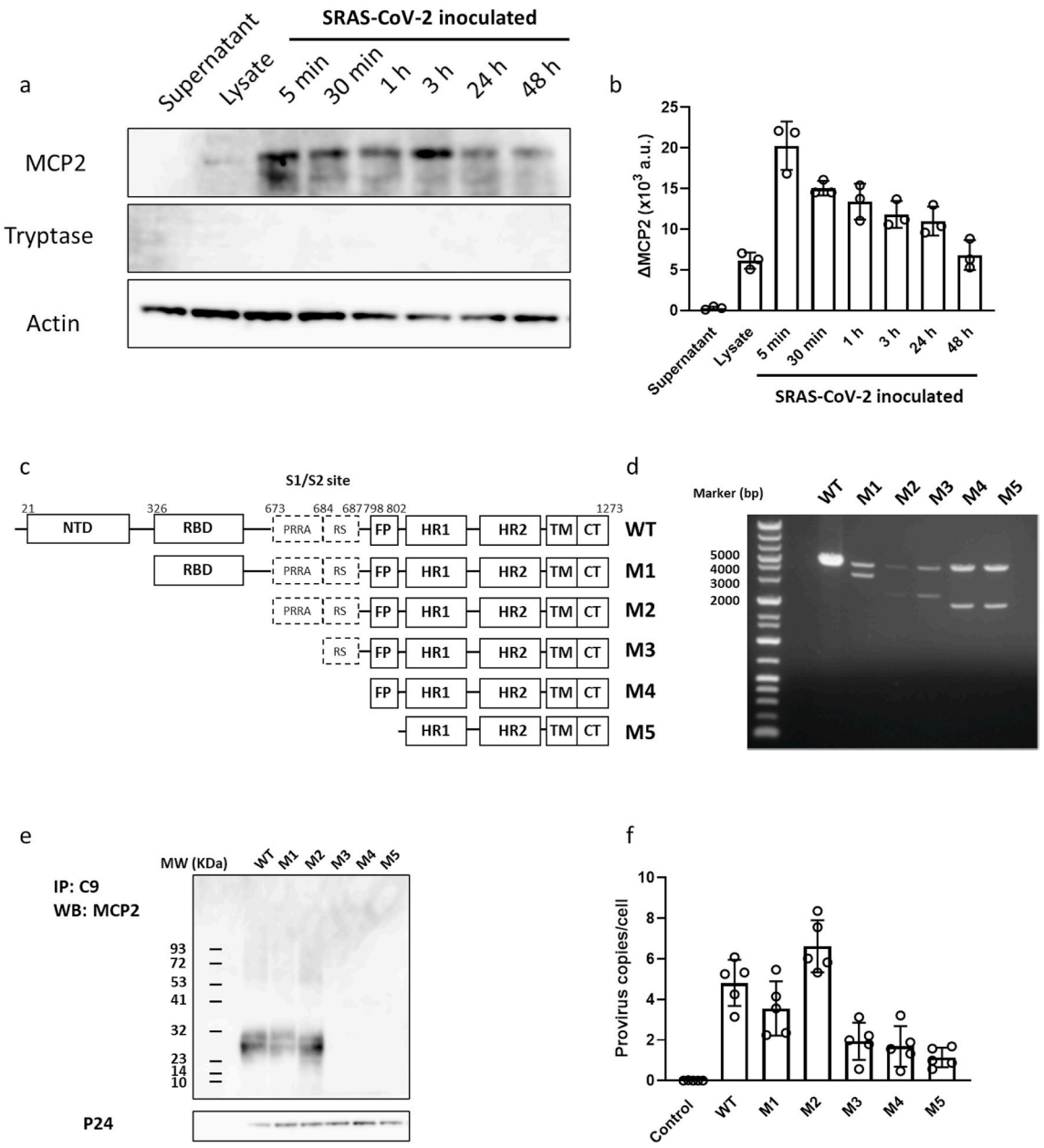

Fig. 2. Mast cell-derived MCP2 formed a complex with SARS-CoV-2 spike protein. (a) MCP2 and tryptase protein, which was co-immunoprecipitated using a specific antibody for spike glycoprotein of SARS-CoV-2, was detected using western blotting. RBL-2H3 cells were inoculated with pseudovirions of SARS-CoV-2 S, and protein levels were determined at the indicated time points. Upper: Expression of MCP2 in culture supernatant (lane 1), cell lysate (lane 2) of non-activated RBL-2H3 cells, and supernatant of virus-inoculated RBL-2H3 cells, which was co-immunoprecipitated with spike glycoprotein of SARS-CoV-2 at the indicated time points (lane 3–8). Middle: Expression of tryptase in each sample as described above. Lower: Expression of actin which served as a loading control. (b) Expression of MCP2 and tryptase protein levels was normalized against actin level in total cell lysates (a,u., arbitrary units). (c) Diagram of wild-type SARS-CoV-2 S protein (WT) and its truncations (M1-5). (d) The inserted fragments of reconstructed plasmids of pcDNA3.1-SARS2-S (WT), pcDNA3.1-SARS2-S1-NTD (M1), pcDNA3.1-SARS2-S1-RBD (M2), pcDNA3.1-SARS2-S1-S2 (M3), pcDNA3.1-SARS2-L (M4), and pcDNA3.1-SARS2-FP (M5) were confirmed by restriction enzyme digestion following by agarose separation. These plasmids were used for pseudovirions and production of mutations in the following experiments. (e) MCP2 protein in culture supernatant of virus-inoculated RBL-2H3 cells, which was co-immunoprecipitated using a specific antibody for C9-tag of spike glycoprotein of SARS-CoV-2, was detected using western blotting. Upper: MCP2 which was co-immunoprecipitated with C9-tag of SARS-CoV-2 (lane 1) and its mutations (lane 1–5). Lower: Expression of virus-derived p24 served as a loading control. (f) The number of integrated provirus copies in RBL-2H3 cells was determined 72 h post-inoculation of either SARS-CoV-2 S or its mutants (n = 5). Values are presented as the scatter plot of individual values with mean ± SD.

3.4. Mast cells and MCP2 facilitate viral entry into respiratory system in acute phase of infection

To further evaluate the role of mast cells and MCP2 in systemic viral entry, we inoculated either male mast cell-deficient WBB6F1/Kit-Kit^{W}/$Kit^{W\text{-}v}$ mice or wild-type C57BL/6JJms mice via the intranasal route with 5×10^6 IFU SARS-CoV-2 S pseudovirions. Viral entry into nose, bronchus, and lung mucosal cells, and peripheral blood was evaluated in both the acute phase (3d) and late-phase (7d) post-viral inoculation (Fig. 4). Compared to wild-type mice, viral entry was suppressed in the nose and bronchus in Kit^{W}/$Kit^{W\text{-}v}$ mice, while significantly elevated viral entry was detected in the lung 3 days after viral inoculation. In the late-phase post-inoculation, higher levels of viral entry were observed in the respiratory tract, including the nasal mucosa, bronchus and lung of mast

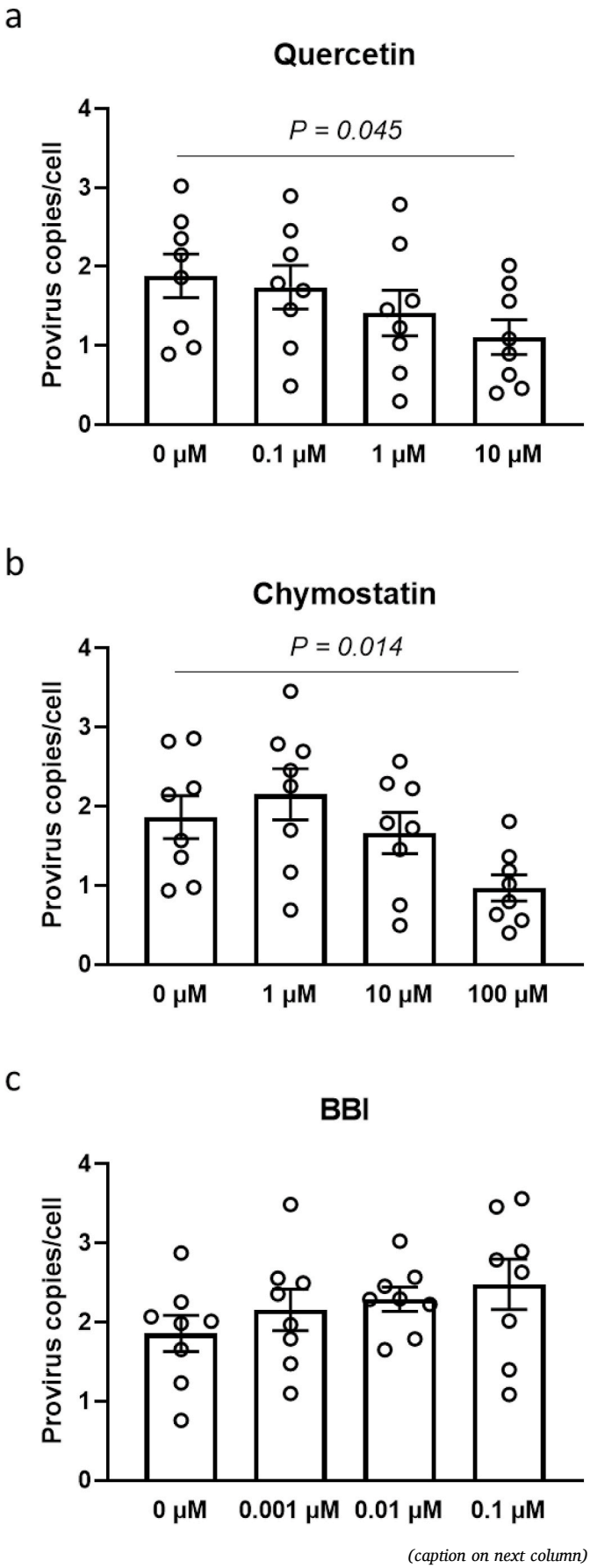

(caption on next column)

Fig. 3. Efficacy of potential mast cell inhibitors on viral entry of SARS-CoV-2. Wild-type pseudovirions of SARS-CoV-2 S were inoculated into a HEK293 T-RBL-2H3 cell coculture system *in vitro*. Cells were pretreated with (a) quercetin, (b) chymostatin, or (c) Bowman-Birk protease inhibitor (BBI) before virus inoculation. The number of integrated provirus copies in RBL-2H3 cells was determined 72 h post-inoculation (n = 8). Values are presented as the scatter plot of individual values with mean ± SD.

cell-deficient mice compared to wild-type mice. Viral entry was localized in the respiratory system, and an extremely low level of genomic integration was observed in peripheral blood in both the acute and late phase post-viral inoculation. These results suggest that the absence of mast cells may influence the viral uptake of upper respiratory tract cells, which consequently increases the risk of viral invasion into the lower respiratory tract. Furthermore, mast cell-deficient mice exhibited ongoing infection in the late phase post-viral inoculation.

To investigate the potential impact of MCP2 on viral entry, SARS-CoV-2 S pseudovirions were pretreated with activated MCP2. In the acute phase post-inoculation, MCP2-pretreated pseudovirions exhibited higher infective ability, especially in the lung, compared with non-treated pseudovirions. Interestingly, 7 days after viral inoculation, a significant decrease in integrated viral genome was observed in the entire respiratory tract, including the nasal mucosa, bronchus, and lung. These results indicate that pre-treatment with MCP2 accelerates viral uptake in the acute phase post-viral inoculation, but may contribute to viral clearance in the late phase post-inoculation.

4. Discussion

Resident mucosal mast cells are likely to be an early target of SARS-CoV-2 infection as they are prevalent in the respiratory mucosa, localize in nearby blood vessels, and accumulate at sites of inflammation. Here, we made a primary attempt to elucidate the effects of SARS-CoV-2 inoculation on mast cells, which may contribute as host antiviral factors in viral infections. Extracellular mast cell-derived mediators, focusing on MCP2 in the current study, play a critical role in viral entry via interaction with viral spike protein. The formation of MCP2/spike complex may trigger protease-dependent syncytium formation and impact on early-phase infection and later systemic spread of SARS-CoV-2.

Processing of viral glycoproteins by host cell proteases can have several consequences, which increase or can be essential for viral infectivity (Glowacka et al., 2011). The cleavage can result in glycoprotein shedding, and the shed proteins can act as antibody decoys or modulate cellular functions by binding to host cell receptors. In the current study, exposure to SARS-CoV-2 pseudovirions triggered mast cell activation and promoted viral entry into HEK293 T cells via released cellular mediators. A hypothesis of a potential relationship between mast cell-derived serine proteases and enhanced infectivity of SARS-CoV-2 has emerged. RBL-2H3 cells, the mast cell line used in the present *in vitro* study, are rat mucosal type-like mast cells that have extremely low expression of ectoenzyme ACE 2 and none of the eight rat tryptase genes are expressed in these cells (Shim et al., 2019). MCP2, a rodent specific β-chymase initially expressed in RBL-2H3 cells, acts as a dominant AT I-hydrolyzing enzyme and generates AT II in these cells (Caughey et al., 2000). Our immunoprecipitation results validate that truncated pseudovirions undergo an activity-dependent interaction with rMCP2, which could activate SARS-CoV-2 S protein and lead to membrane fusion. The lack of binding property of a truncated mutant pseudovirion with a deletion of the S1/S2 junction indicates that this furin cleavage motif could be a potential functional site of MCP2 on SARS-CoV-2 S protein. Additionally, MCP2 processes chymotrypsin-like cleavage specificity. It cleaves the C-terminal side of proteins after aromatic amino acids such as Phe, Tyr and Trp as the preferred amino acids in general (Caughey et al., 2000). Combined with data concerning peptide substrate cleavage preferences, structure basis observation has

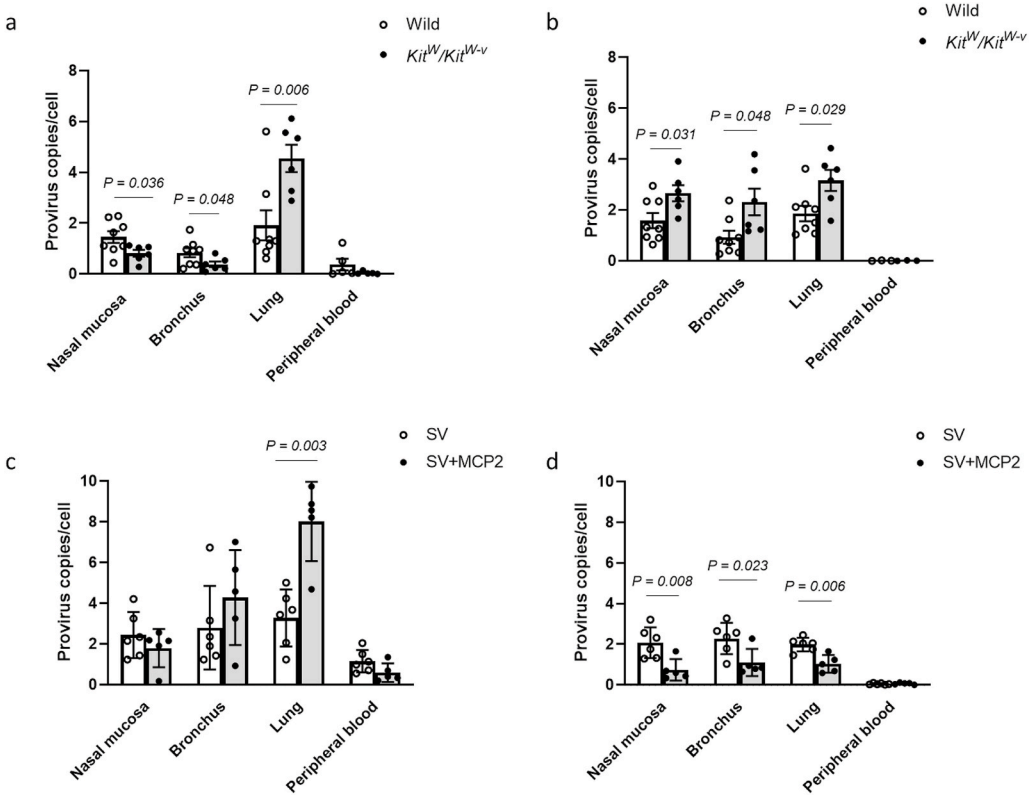

Fig. 4. Investigation of contribution of mast cells and MCP2 to viral entry *in vivo*. Both mast cell-deficient WBB6F1/Kit-Kit^W/Kit^{W-v} mice and wild control C57BL/6JJms mice were inoculated intranasally with 20 μL SARS-CoV-2 S pseudovirions (5×10^6 TCID50). The number of integrated provirus copies was determined on (a) day 3 and (b) day 7 after virus inoculation (n = 6–8). SARS-CoV-2 S pseudovirions, which were pretreated with MCP2, were also intranasally inoculated into wild-type mice. The number of integrated provirus copies was determined on (c) day 3 and (d) day 7 after virus inoculation (n = 6–8). Values are presented as the scatter plot of individual values with mean ± SD.

enabled predictions of functional cleavage of MCP2 on the furin site as with other serine proteases, such as TMPRSS2. Although functional cleavage of spike protein by MCP2 has not been successfully demonstrated yet, the inhibitory effect of chymostatin on viral entry indicates the potential impact of mast cell-derived MCP2 on viral entry. Elucidation of the favorable kinetics of the MCP2-spike interaction and the catalytic efficiency of MCP-2 will be the focus of our future studies.

MCP 2-expressing mast cells, so-called mucosal mast cells, in contrast to connective tissue mast cells which specifically express tryptase, are the dominant subtype on the mucosal surface of the human respiratory tract (Andersson et al., 2009). Why mucosal mast cells, as a protective innate immune cell, promote viral entry into themselves and other peripheral resident cells would be the next interesting issue to explore. Our studies on SARS-CoV-2 pseudovirion infection in mast cell-deficient mice revealed decreased viral entry into the upper respiratory tract in the absence of mast cells in the early stage after viral inoculation, in contrast to enhanced infection in the lung. Furthermore, in the late-phase response after viral inoculation, relatively higher copies of integrated virus remained in the entire respiratory tract in mast cell-deficient mice compared to wild-type mice. Therefore, localized mast cell responses to SARS-CoV-2 seem to be protective by 'trapping' the virus via promoting cell loading to avoid viral spread to the lower respiratory tract in the early phase of viral infection, which may contribute to viral clearance in the later post-infection phase.

In the early phase of anti-viral responsiveness, viral loading could evade mast cell phagocytic killing by entering into a compartment within the mast cell that bypasses phagolysosomal fusion and affects viral survival, as reported in other types of pathogenic infection, such as bacteria (Dudeck et al., 2019). Besides intracellular killing activity, the contribution of peripheral cells to viral intake could facilitate systemic later viral clearance activities by sensing danger signals released from infected cells (alarmins) and mediators produced in the context of antiviral responses (cytokines and interferons), resulting in the recruitment and conditioning of additional effector cells, such as natural killer cells, macrophages, and $CD8^+$ T cells (Dudeck et al., 2019; Podlech et al., 2015). Without rapid sensing of mast cells and promotion of secondary effector cell infiltration into the respiratory tract, as demonstrated in murine cytomegalovirus-infected mast cell-deficient mice, markedly more severe signs of infection were observed in mast cell-deficient mice compared to wild-type mice (Ebert et al., 2014). The protective contribution of mast cells and their pro-inflammatory mediators was demonstrated by previous evidence and the findings of the present study.

On the other hand, based on current knowledge, excessive responses of mast cells are correlated with the severity of coronavirus infection and subsequent systemic cytokine storm (Conti et al., 2020; Theoharides, 2021). Clinically, mast cell activation with a serum elevation of MCP2 has been confirmed in COVID-19 patients (Tan et al., 2021). An integrated treatment approach addressing mast cells and their pro-inflammatory mediators, including combined administration of a natural flavanol, quercetin, the structurally related flavone, luteolin, and other anti-inflammatory agents, appeared to be quite effective in the treatment of patients with severe COVID-19 infection (Theoharides et al., 2022). Our *in vitro* observations also support the findings in clinical practice. We tested the efficacy of a mast cell membrane stabilizer (quercetin) and chymase inhibitors (chymostatin and BBI) on the point of viral entry. Quercetin and chymostatin inhibited viral entry into mast cell-cocultured HEK293 cells at relatively high dosages (10 and 100 μM, respectively), whereas BBI did not affect viral entry. Furthermore, *in vivo,* MCP2-pretreated pseudovirions exhibited higher infective ability, especially in the lung, compared with non-treated pseudovirions. Although we are not able to assess the impact of the efficacy of these inhibitors in the treatment of pulmonary symptoms *in vivo* using our current pseudovirus-infected model, in which the pathological presence of COVID-19 cannot be reproduced without viral multiplication, blockade of mast cell activity or MCP2 does inhibit mast cell-promoted viral entry *in vitro*.

Therefore, the next speculation would be, should we eliminate mast cell-mediated viral entry in the management of COVID-19 pneumonia? Considering the protective effects of mast cells and MCP2, it can be

argued that as an initiative, mast cell stabilizers and chymase inhibitors could be used. Since mast cell activities sense the risk of viral invasion and trigger a host antiviral systemic response, it seems less necessary to be given as prophylactic administration or in patients right after testing positive for COVID-19 and in patients showing only minor symptoms. Mast cell stabilizers and chymase inhibitors should be considered in patients at high risk of cytokine storm, such as those with a high viral load or high serum levels of interleukin 6 and C-reactive protein (Shcherbak et al., 2021).

In conclusion, the current work dissected the responses of mast cells to SARS-CoV-2 from the host defense viewpoint, using a pseudoviral system. Formation of viral spike/MCP2 complex may promote viral entry into mast cells themselves and other peripheral cells. Because both protective effects and pathogenic influences of virus-triggered mast cells were observed, mast cells emerge as multifaceted immune modulators and operators at the interfaces of viral invasion. Further studies are needed to clarify how to manage the actions of mast cells and their mediators toward an advantageous outcome in COVID-19 treatment.

Declaration of competing interest

The authors declare that the research was conducted in the absence of any commercial or financial relationship that could be construed as a potential conflict of interest.

CRediT authorship contribution statement

Shuang Liu: Conceptualization, Methodology, Formal analysis, Writing – original draft. **Yasuyuki Suzuki:** Conceptualization, Writing – review & editing, Validation. **Erika Takemasa:** Investigation, Resources. **Ryusuke Watanabe:** Conceptualization, Writing – review & editing. **Masaki Mogi:** Supervision, Project administration, Funding.

Data availability

Data will be made available on request.

References

Andersson, C.K., Mori, M., Bjermer, L., Löfdahl, C.G., Erjefält, J.S., 2009. Novel site-specific mast cell subpopulations in the human lung. Thorax 64, 297–305.

Caughey, G.H., Raymond, W.W., Wolters, P.J., 2000. Angiotensin II generation by mast cell alpha- and beta-chymases. Biochim. Biophys. Acta 1480, 245–257.

Chan, J.F., Kok, K.H., Zhu, Z., Chu, H., To, K.K., Yuan, S., Yuen, K.Y., 2020. Genomic characterization of the 2019 novel human-pathogenic coronavirus isolated from a patient with atypical pneumonia after visiting Wuhan. Emerg. Microb. Infect. 9, 221–236.

Conti, P., Caraffa, A., Tetè, G., Gallenga, C.E., Ross, R., Kritas, S.K., Frydas, I., Younes, A., Di Emidio, P., Ronconi, G., 2020. Mast cells activated by SARS-CoV-2 release histamine which increases IL-1 levels causing cytokine storm and inflammatory reaction in COVID-19. J Biol Regul Homeost Agents. Copyright 2020 Biolife Sas 1629–1632. Italy. www.biolifesas.org.

Dudeck, A., Köberle, M., Goldmann, O., Meyer, N., Dudeck, J., Lemmens, S., Rohde, M., Roldán, N.G., Dietze-Schwonberg, K., Orinska, Z., Medina, E., Hendrix, S., Metz, M., Zenclussen, A.C., von Stebut, E., Biedermann, T., 2019. Mast cells as protectors of health. J. Allergy Clin. Immunol. 144, S4–s18.

Ebert, S., Becker, M., Lemmermann, N.A., Büttner, J.K., Michel, A., Taube, C., Podlech, J., Böhm, V., Freitag, K., Thomas, D., Holtappels, R., Reddehase, M.J., Stassen, M., 2014. Mast cells expedite control of pulmonary murine cytomegalovirus infection by enhancing the recruitment of protective CD8 T cells to the lungs. PLoS Pathog. 10, e1004100.

Glowacka, I., Bertram, S., Müller, M.A., Allen, P., Soilleux, E., Pfefferle, S., Steffen, I., Tsegaye, T.S., He, Y., Gnirss, K., Niemeyer, D., Schneider, H., Drosten, C., Pöhlmann, S., 2011. Evidence that TMPRSS2 activates the severe acute respiratory syndrome coronavirus spike protein for membrane fusion and reduces viral control by the humoral immune response. J. Virol. 85, 4122–4134.

He, S., Gaça, M.D., McEuen, A.R., Walls, A.F., 1999. Inhibitors of chymase as mast cell-stabilizing agents: contribution of chymase in the activation of human mast cells. J. Pharmacol. Exp. Therapeut. 291, 517–523.

Huang, Y., Yang, C., Xu, X.F., Xu, W., Liu, S.W., 2020. Structural and functional properties of SARS-CoV-2 spike protein: potential antivirus drug development for COVID-19. Acta Pharmacol. Sin. 41, 1141–1149.

Kempuraj, D., Selvakumar, G.P., Ahmed, M.E., Raikwar, S.P., Thangavel, R., Khan, A., Zaheer, S.A., Iyer, S.S., Burton, C., James, D., Zaheer, A., 2020. COVID-19, mast cells, cytokine storm, psychological stress, and neuroinflammation. Neuroscientist 26, 402–414.

Kritas, S.K., Ronconi, G., Caraffa, A., Gallenga, C.E., Ross, R., Conti, P., 2020. Mast cells contribute to coronavirus-induced inflammation: new anti-inflammatory strategy. J Biol Regul Homeost Agents. Copyright 2019 Biolife Sas 9–14. Italy. www.biolifesas.org.

Letko, M., Marzi, A., Munster, V., 2020. Functional assessment of cell entry and receptor usage for SARS-CoV-2 and other lineage B betacoronaviruses. Nat Microbiol 5, 562–569.

Liu, S., Sahid, M.N., Takemasa, E., Kiyoi, T., Kuno, M., Oshima, Y., Maeyama, K., 2016. CRACM3 regulates the stability of non-excitable exocytotic vesicle fusion pores in a Ca(2+)-independent manner via molecular interaction with syntaxin4. Sci. Rep. 6, 28133.

Liu, S., Sahid, M.N.A., Takemasa, E., Maeyama, K., Mogi, M., 2018. Zoledronate modulates intracellular vesicle trafficking in mast cells via disturbing the interaction of myosinVa/Rab3a and sytaxin4/VAMP7. Biochem. Pharmacol. 151, 18–25.

Morrison, J., Rathore, A.P.S., Mantri, C.K., Aman, S.A.B., Nishida, A., St John, A.L., 2017. Transcriptional profiling confirms the therapeutic effects of mast cell stabilization in a dengue disease model. J. Virol. 91.

Ou, X., Liu, Y., Lei, X., Li, P., Mi, D., Ren, L., Guo, L., Guo, R., Chen, T., Hu, J., Xiang, Z., Mu, Z., Chen, X., Chen, J., Hu, K., Jin, Q., Wang, J., Qian, Z., 2020. Characterization of spike glycoprotein of SARS-CoV-2 on virus entry and its immune cross-reactivity with SARS-CoV. Nat. Commun. 11, 1620.

Podlech, J., Ebert, S., Becker, M., Reddehase, M.J., Stassen, M., Lemmermann, N.A., 2015. Mast cells: innate attractors recruiting protective CD8 T cells to sites of cytomegalovirus infection. Med. Microbiol. Immunol. 204, 327–334.

Senyshyn, J., Baumgartner, R.A., Beaven, M.A., 1998. Quercetin sensitizes RBL-2H3 cells to polybasic mast cell secretagogues through increased expression of Gi GTP-binding proteins linked to a phospholipase C signaling pathway. J. Immunol. 160, 5136–5144.

Shcherbak, S.G., Anisenkova, A.Y., Mosenko, S.V., Glotov, O.S., Chernov, A.N., Apalko, S. V., Urazov, S.P., Garbuzov, E.Y., Khobotnikov, D.N., Klitsenko, O.A., Minina, E.M., Asaulenko, Z.P., 2021. Basic predictive risk factors for cytokine storms in COVID-19 patients. Front. Immunol. 12, 745515.

Shim, J.K., Kennedy, R.H., Weatherly, L.M., Abovian, A.V., Hashmi, H.N., Rajaei, A., Gosse, J.A., 2019. Searching for tryptase in the RBL-2H3 mast cell model: preparation for comparative mast cell toxicology studies with zebrafish. J. Appl. Toxicol. 39, 473–484.

Tan, J., Anderson, D.E., Rathore, A.P.S., O'Neill, A., Mantri, C.K., Saron, W.A.A., Lee, C., Cui, C.W., Kang, A.E.Z., Foo, R., Kalimuddin, S., Low, J.G., Ho, L., Tambyah, P., Burke, T.W., Woods, C.W., Chan, K.R., Karhausen, J., John, A.L.S., 2021. Signatures of Mast Cell Activation Are Associated with Severe COVID-19. medRxiv.

Theoharides, T.C., 2021. Potential association of mast cells with coronavirus disease 2019. Ann. Allergy Asthma Immunol. 126, 217–218.

Theoharides, T.C., Alysandratos, K.D., Angelidou, A., Delivanis, D.A., Sismanopoulos, N., Zhang, B., Asadi, S., Vasiadi, M., Weng, Z., Miniati, A., Kalogeromitros, D., 2012. Mast cells and inflammation. Biochim. Biophys. Acta 1822, 21–33.

Theoharides, T.C., Guerra, L., Patel, K., 2022. Successful treatment of a severe COVID-19 patient using an integrated approach addressing mast cells and their mediators. Int. J. Infect. Dis. 118, 164–166.

Ware, J.H., Wan, X.S., Rubin, H., Schechter, N.M., Kennedy, A.R., 1997. Soybean Bowman-Birk protease inhibitor is a highly effective inhibitor of human mast cell chymase. Arch. Biochem. Biophys. 344, 133–138.

Xia, S., Zhu, Y., Liu, M., Lan, Q., Xu, W., Wu, Y., Ying, T., Liu, S., Shi, Z., Jiang, S., Lu, L., 2020. Fusion mechanism of 2019-nCoV and fusion inhibitors targeting HR1 domain in spike protein. Cell. Mol. Immunol. 17, 765–767.